P. E. Phelan[1]
e-mail: phelan@asu.edu

Y. Gupta

H. Tyagi[2]
Assistant Professor

R. S. Prasher[3]

Department of Mechanical and Aerospace Engineering,
Arizona State University,
Tempe, AZ

J. Catano

G. Michna[4]
Assistant Professor

R. Zhou

J. Wen[5]

M. Jensen

Y. Peles

Department of Mechanical, Aerospace and Nuclear Engineering,
Rensselaer Polytechnic University,
Troy, NY

Energy Efficiency of Refrigeration Systems for High-Heat-Flux Microelectronics

Increasingly, military and civilian applications of electronics require extremely high-heat fluxes on the order of 1000 W/cm^2. Thermal management solutions for these severe operating conditions are subject to a number of constraints, including energy consumption, controllability, and the volume or size of the package. Calculations indicate that the only possible approach to meeting this heat flux condition, while maintaining the chip temperature below 65°C, is to utilize refrigeration. Here, we report an initial thermodynamic optimization of the refrigeration system design. In order to hold the outlet quality of the fluid leaving the evaporator to less than approximately 20%, in order to avoid reaching critical heat flux, the refrigeration system design is dramatically different from typical configurations for household applications. In short, a simple vapor-compression cycle will require excessive energy consumption, largely because of the additional heat required to return the refrigerant to its vapor state before the compressor inlet. A better design is determined to be a "two-loop" cycle, in which the vapor-compression loop is coupled thermally to a pumped loop that directly cools the high-heat-flux chip.
[DOI: 10.1115/1.4003041]

1 Introduction

The removal of very high-heat fluxes, up to 1000 W/cm^2, is required by some military and commercial electronics applications. Simultaneously, usually the electronic device temperature must be maintained below some threshold value, such as 65°C. The combination of an extremely high-heat flux removal and low device temperatures necessitates the use of refrigeration to maintain satisfactory performance.

Several groups have investigated refrigeration cooling of electronic systems. A number of studies have examined how miniature, often termed *mesoscale*, refrigeration systems may be utilized for microelectronics cooling (see, e.g., Refs. [1–5]). A general review of electronics cooling approaches was given in Ref. [6]. Somewhat larger vapor-compression systems are already commercially available for desktop computers [7] and remain the object of study [8]. These systems are essentially conventional vapor-compression refrigerators applied to electronics cooling for the purposes of maintaining low operating temperatures and generally do not involve the removal of extremely high-heat fluxes.

In contrast, our focus here is on the design of macroscale vapor-compression refrigeration systems for *high-heat-flux* microelectronic systems. Such systems are of considerable interest in the literature (see, e.g., Refs. [9,10]), but these are still largely confined to conventional vapor-compression systems. Our present work shows that when considering the limitations on the evaporator exit quality imposed by critical heat flux (CHF) avoidance, the conventional vapor-compression cycle may not be the optimum choice. We compare a number of alternative system designs and show that the best choice with regard to energy efficiency is a "two-loop" system in which the electronic device is cooled by a pumped loop that is cascaded with a conventional vapor-compression loop. Note that this is in agreement with recent reports that described how a similar two-loop system was utilized for subcooled flow boiling experiments in microchannels [11,12].

2 Analysis

In order to cool the electronic component (chip), several types of refrigeration cycles are envisaged in this study. An evaporator is placed in thermal contact with the chip. This evaporator contains microchannels through which subcooled refrigerant flows. This way the heat from the chip is removed by boiling the refrigerant flowing through the evaporator. In each of these cycles, the refrigerant considered is R-134a.

The following assumptions and constraints are adhered to for most calculations in this study. The refrigerant enters the evaporator as subcooled liquid 10°C less than the evaporator temperature, i.e., subcooled by 10°C. Two values of evaporator temperatures are considered: T_{evap}=0°C and T_{evap}=20°C. These inlet temperatures are based on the estimated value of temperature dif-

[1]Corresponding author.
[2]Present address: School of Mechanical Materials & Energy Engineering, Indian Institute of Technology Ropar, Rupnagar, 140001, Punjab, India.
[3]Also at ARPA-E, Department of Energy, 1000 Independence Ave. SW, Washington, DC 20585.
[4]Present address: South Dakota State University, Mechanical Engineering Department, Crothers Engineering Hall 254, Box 2219, Brookings, SD 57007–0294.
[5]Also at Department of Electrical, Computer, and Systems Engineering, Rensselaer Polytechnic University.
Manuscript received September 11, 2009; final manuscript received November 6, 2010; published online December 16, 2010. Assoc. Editor: Anthony M. Jacobi.

ference between the heater surface and the refrigerant, obtained from Ref. [13], for heat fluxes close to 1000 W/cm^2.

For simplicity, the flow through the evaporator is assumed to undergo no pressure drop. This is done in order to simplify the calculations and to focus on the comparison between the various refrigeration cycles while maintaining similar operating conditions among them. Similarly, the refrigerant exiting from the evaporator is assumed to be limited to a quality of $x=20\%$. This constraint on evaporator exit quality helps to avoid CHF conditions inside the evaporator. The chip is assumed to produce heat at 1 kW, which is transferred completely to the refrigerant flowing in the evaporator.

The exit quality constraint of $x=20\%$ was chosen because of the great uncertainty surrounding the effect of exit quality on CHF. Wojtan et al. [14] observed CHF at $x<40\%$ in a single channel with flowing R-134a. Depending on the mass flux, Koşar and Peles [15] found CHF for R-123 to occur in silicon-based microchannels for exit qualities as low as 25%. On the other hand, a number of studies found that exit qualities could be much higher before CHF was initiated (see the review in Ref. [16] and the references cited within), leading to the statement "…there is no general agreement on the trends in the CHF condition in micro/minichannels so far" [16]. Furthermore, measurements on the flow boiling of R-134a in copper microchannels showed that the peak heat transfer coefficient occurred at a local quality of ~20% [17]. Therefore, we choose to limit the exit quality in the evaporator to only 20% until more information is available that would allow us to confidently operate at higher exit qualities.

Standard steady-state equations are applied to compute the refrigerant mass flow rates and the required power inputs. In all cases, the evaporator heat load is $\dot{Q}_{evap}=1$ kW. All compressors and pumps are assumed to have isentropic efficiencies of 80%, i.e., for the compressors $\eta_{com}=0.8$ and for the pumps $\eta_{pump}=0.8$. The condenser temperature is set at $T_{cond}=40°C$ in all cases. The system coefficient of performance (COP) for each case is defined as

$$\mathrm{COP}=\frac{\dot{Q}_{evap}}{\dot{P}_{in}} \tag{1}$$

where $\dot{P}_{in}$ is the power input required to drive any compressors or pumps in the system plus any additional heating. All computations are carried out in Engineering Equation Solver® (EES). The detailed calculations for each case are given in Sec. 3.

3 Results and Discussion

In this study, four types of R-134a refrigeration cycles are considered. These four cycles are referred to as cycle 1, cycle 2, cycle 3, and cycle 4. Cycle 1 is a conventional vapor-compression refrigeration cycle, cascaded with a second vapor-compression cycle in order to deliver subcooled refrigerant at the evaporator inlet. The cycle 1 schematic diagram is shown in Fig. 1, and a *T-s* (temperature-entropy) diagram for the same cycle is shown in Fig. 2. In this and in the following cycles, the integrated circuit chip transfers its heat to the evaporator and, as discussed above, the exit quality of the refrigerant leaving the evaporator is limited to $x=0.20$. In cycle 1, after leaving the evaporator, the refrigerant flows through an additional heater in order to bring the refrigerant to the saturated vapor condition so that it can enter the compressor. After exiting the compressor, the refrigerant passes through the condenser, which is maintained at a temperature $T_{cond}=40°C$. The subcooler, located after the condenser, subcools the refrigerant 10°C below the evaporator temperature.

As stated above, standard steady-state equations are applied to compute the refrigerant mass flow rates and the required power inputs, which for case 1 is the power required by both compressors and the additional heating required to completely vaporize

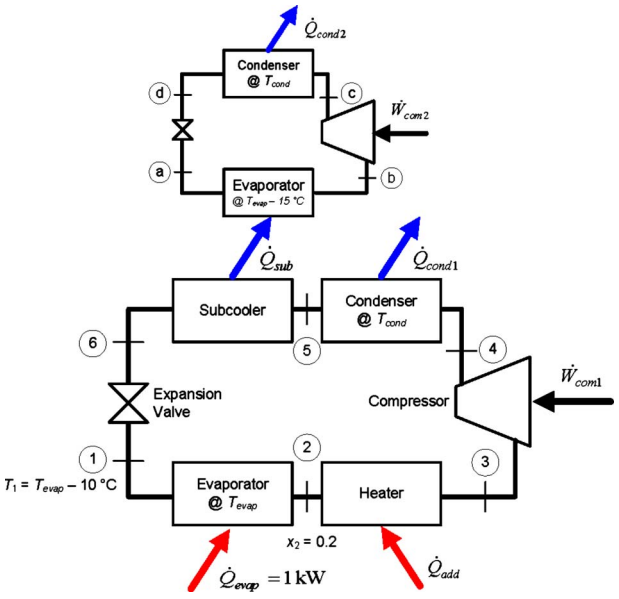

Fig. 1 Schematic diagram of a conventional vapor-compression refrigeration system (cycle 1), with a second vapor-compression cycle cascaded to produce subcooled conditions at the evaporator inlet

the refrigerant leaving the evaporator. The mass flow rate in the primary vapor-compression loop ($\dot{m}$) and in the cascaded loop ($\dot{m}_{sub}$) are found from

$$\dot{m}=\frac{\dot{Q}_{evap}}{h_2-h_1},\quad \dot{m}_{sub}=\frac{\dot{m}(h_5-h_6)}{h_b-h_a} \tag{2}$$

The compressor power inputs are computed from

$$\dot{W}_{com1}=\dot{m}(h_4-h_3),\quad \dot{W}_{com2}=\dot{m}_{sub}(h_c-h_b) \tag{3}$$

Additional details can be found in standard thermodynamics textbooks, such as Ref. [18].

The system in case 1 suffers from two serious drawbacks. The first is the heating power required in the heater following the evaporator to bring the refrigerant to the saturated vapor condition, starting from the evaporator exit quality of $x=20\%$. For

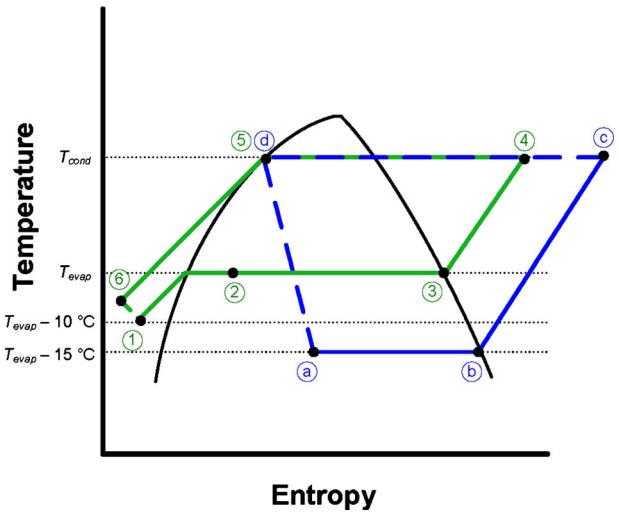

Fig. 2 *T-s* (temperature-entropy) diagram for cycle 1 (conventional vapor-compression cycle cascaded with a second vapor-compression cycle)

Table 1 Comparison among the four cycles considered for the refrigeration system design (T_{evap}=0°C, T_{cond}=40°C, 10°C of subcooling)

Cycle No. and description	Net electric power consumption (kW)	System COP	Advantages/ disadvantages
1: Cascaded vapor-compression	4.08	0.245	• High power consumption • Difficult to control • Potential for heat recovery from condensers and/or compressors
2: Vapor compression with economizer	2.41	0.415	• Moderate power consumption • Difficult to control • Relatively simple design • Potential for heat recovery from condenser and/or compressor
3: Pumped loop with thermoelectric cooler	5.53	0.181	• Highest power consumption • Large number of thermoelectric modules required • Simplest design • Easy to control
4: Pumped loop with vapor-compression (two-loop)	0.43	2.35	• Lowest power consumption • Easy to control • Compressor loop is commercial off-the-shelf (COTS) • Relatively simple design

T_{evap}=0°C, the additional heat added is $\dot{Q}_{add}$=3.00 kW, compared with compressor power inputs of $\dot{W}_{com1}$=0.610 kW and $\dot{W}_{com1}$=0.469 kW, leading to COP=$\dot{Q}_{evap}/(\dot{W}_{com1}+\dot{W}_{com2}+\dot{Q}_{add})$=0.245. Second, there are inherent difficulties to control the system to adjust to varying evaporator heat loads. The compressor speed can be varied, but care must be taken to ensure that 100% vapor enters the compressor. On the other hand, an opportunity exists for heat recovery from either compressor, or even from the condensers, in order to reduce the additional heat requirement. Implementing such a heat recovery scheme, though, would add complexity that might detract from the gains in energy efficiency. A summary of the calculated power input and COP, plus a listing of apparent advantages and disadvantages, is provided in Table 1 for each of the four cycles.

In order to address the challenges that arose in cycle 1, some changes were made to the refrigeration cycle, and as a result cycle 2 was envisioned. Figure 3 shows the schematic of cycle 2, where an economizer is introduced, as well as a second expansion valve that enables subcooled conditions at the evaporator inlet. The economizer is a heat exchanger between the high-temperature liquid exiting the condenser and the liquid/vapor mixture leaving the evaporator. It reduces the additional heat required to $\dot{Q}_{add}$=1.51 kW (T_{evap}=0°C), as shown in the *T-s* diagram in Fig. 4. The system COP is consequently raised to COP=$\dot{Q}_{evap}/(\dot{W}_{com}+\dot{Q}_{add})$=0.415. Importantly, the complexity of the system is reduced since now there is only a single refrigerant compressor, but it is still difficult to control the system to adjust to rapidly varying evaporator heat loads.

Another concept was introduced to address the cooling of the refrigerant, this time by incorporating a thermoelectric cooler (Peltier device) instead of a conventional vapor-compression cycle. The schematic diagram of cycle 3 is given in Fig. 5, and the accompanying *T-s* diagram is given in Fig. 6. Now, the relatively power-hungry compressor is replaced with a pump that consumes much less power, but the low efficiency of the thermoelectric cooler also has to be taken into account. The COP of a thermoelectric cooler, COP_{tec}, is given by [1]

$$COP_{tec} = \frac{\dot{Q}_{tec}}{\dot{W}_{tec}} = \frac{\frac{1}{2}ZT_c^2 - (T_h - T_c)}{ZT_cT_h} \tag{4}$$

where $\dot{Q}_{tec}=\dot{m}(h_3-h_4)$ is the heat load on the thermoelectric cooler, $\dot{W}_{tec}$ is the power input to the thermoelectric cooler, Z is the thermoelectric figure of merit, T_c is the cold temperature experienced by the thermoelectric cooler, and T_h is the hot temperature to which the thermoelectric cooler rejects heat. For bismuth telluride (Bi_2Te_3), $Z(300\ K)\approx 1$ [19], giving $Z\approx 1/300=0.0033\ K^{-1}$. The corresponding system COP is COP

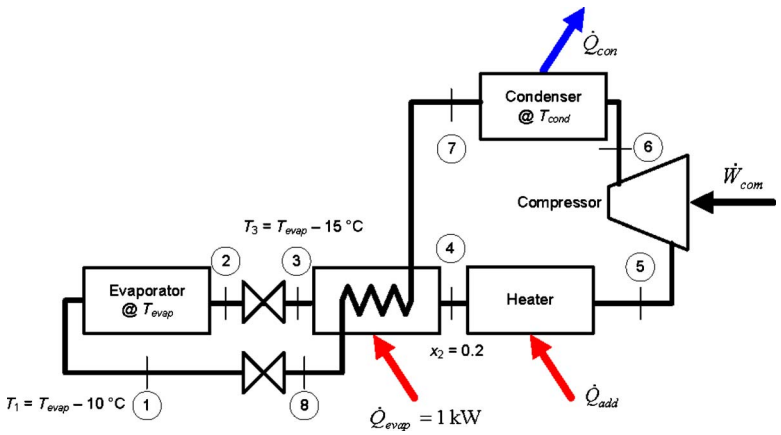

Fig. 3 Schematic diagram of a vapor-compression refrigeration system with economizer (cycle 2)

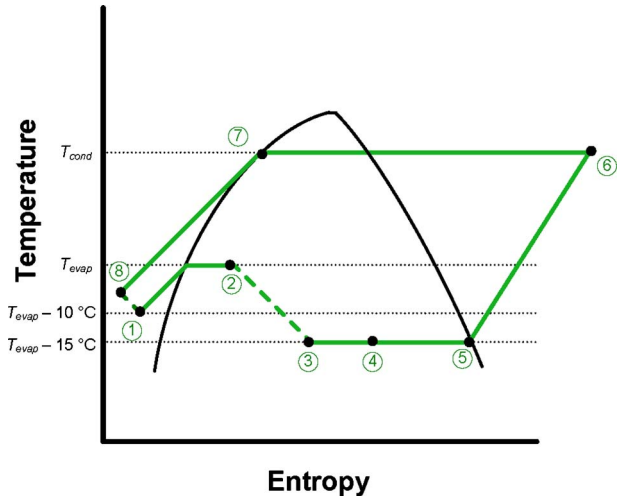

Fig. 4 *T-s* (temperature-entropy) diagram for cycle 2 (conventional vapor-compression cycle with an economizer heat exchanger)

$=\dot{Q}_{evap}/(\dot{W}_{tec}+\dot{W}_{pump})=0.181$, where $T_h=T_{cond}=40°C$ and $T_c=-15°C$. This value of COP is the lowest of the four systems considered because of the large power requirement of the thermoelectric cooler ($\dot{W}_{tec}=5.41$ kW) compared with a pump input power of only $\dot{W}_{pump}=0.124$ kW. Without a compressor, there is no need to add heat to completely vaporize the refrigerant at the evaporator exit, but this is more than offset by $\dot{W}_{tec}$. Still, this system may be attractive for some applications because of its simplicity. Furthermore, it can easily be controlled by varying the pump speed, an advantage also enjoyed by the fourth and final refrigeration system examined, case 4.

Finally, after analyzing the previous three cycles, one last type of cycle was envisaged. This cycle, referred to as cycle 4, utilizes a "two-loop" approach and is shown in Fig. 7. The corresponding *T-s* diagram for this cycle is shown in Fig. 8. A conventional vapor-compression cycle (the "compressor" loop) is cascaded with a "pump" loop that directly cools the electronic chip. Similar to case 3 with the thermoelectric cooler, no additional heating of the refrigerant is required. As a result, this type of cycle consumes the lowest power of the four cycles (0.425 kW), including the compressor ($\dot{W}_{com}=0.375$ kW) and the pump ($\dot{W}_{pump}=0.050$ kW), and is clearly the best among the four cycles from an energy point of view.

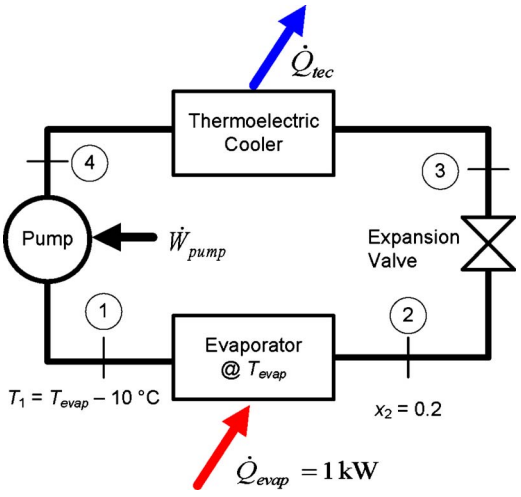

Fig. 5 Schematic diagram of a pumped-loop system cooled by a thermoelectric cooler (cycle 3)

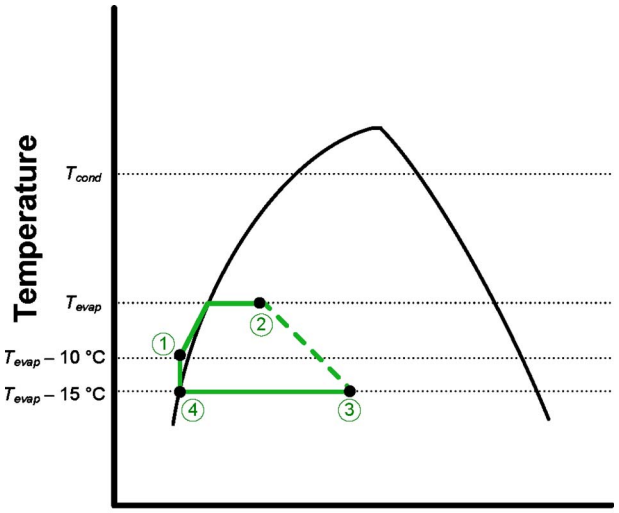

Fig. 6 *T-s* (temperature-entropy) diagram for cycle 3 (pumped loop with thermoelectric cooler)

Other advantages, in addition to dramatically reduced power consumption, are also inherent in the "two-loop" system (cycle 4)

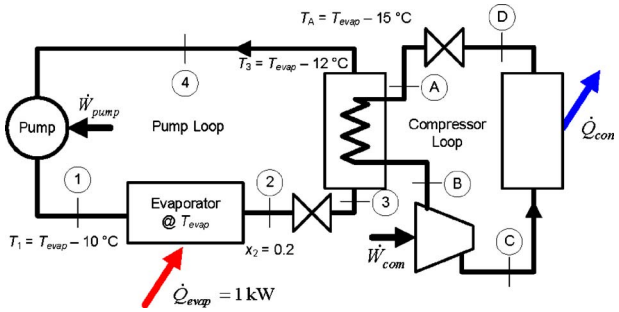

Fig. 7 Schematic diagram of a two-loop system (cycle 4)

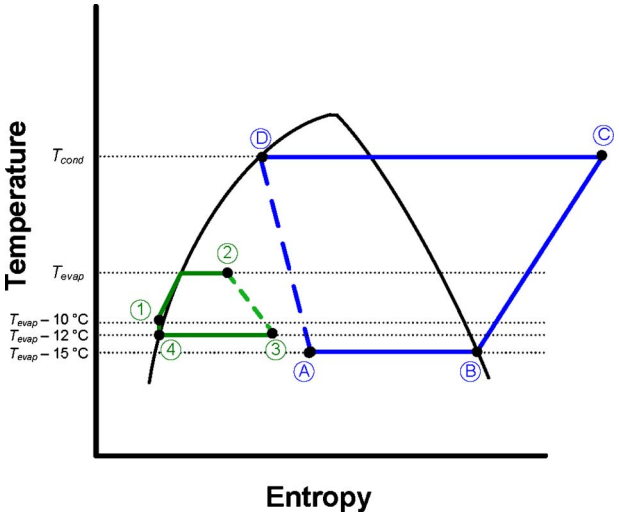

Fig. 8 *T-s* (temperature-entropy) diagram for cycle 4 (two-loop system)

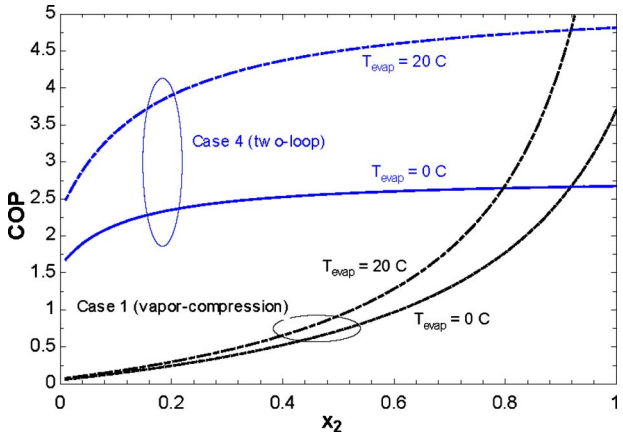

Fig. 9 Comparison of the single-loop (case 1) and two-loop (case 4) configurations based on COP for two different evaporator temperatures (T_{cond}=40°C)

compared with the others. The compressor loop can be a commercially available "off-the-shelf" system, making it low cost and highly reliable. In the pump loop, the choice of refrigerant is no longer tied to the compressor design. Rather, one is free to select any refrigerant with desirable properties, such as high critical heat flux. Furthermore, the range of operating pressures in the pump loop can be made much larger than for vapor-compression cycles since the pressure rise is accomplished via an inexpensive pump rather than by an energy-intensive compressor. Finally, it appears easier to control the pump loop to operate under transient conditions compared with controlling a vapor-compression loop. The pump speed and expansion valve opening can both be rapidly varied to produce different evaporator conditions without compromising the integrity of the system or damaging any components. We will explore the controllability and other aspects, such as optimum refrigerant choice, of the cycle 4 system in future work. For example, the expansion valve in the pump loop is not essential and can possibly be removed to simplify the system.

For high-heat flux electronics cooling, the two-loop system (cycle 4) performs better than the conventional vapor-compression system (cycle 1) or the other two systems investigated. However, it is recognized that, above some evaporator exit quality, the power consumption reduction enjoyed by the two-loop (case 4) system becomes insignificant. Thus, there has to be a critical evaporator exit quality where the use of a conventional vapor-compression system may be a better choice. Figure 9 shows a comparison of the COP for the conventional vapor-compression system (case 1) and the two-loop configuration (case 4) for various exit qualities. Two values of evaporator temperature are considered: T_{evap}=0°C (which has been used in all previous calculations) and T_{evap}=20°C. It is seen that the two-loop system is more efficient than the conventional system up to an exit quality of $x \sim 0.9$ for T_{evap}=0°C and up to $x \sim 0.8$ for T_{evap}=20°C. Thus, for very high evaporator exit qualities, the two-loop system (case 4) loses its energy efficiency advantages relative to a conventional vapor-compression system, but it still offers an advantage in being easier to control for varying evaporator heat loads.

4 Conclusions

Four different types of refrigeration systems were evaluated for their potential to cool a high-heat-flux electronic component. The primary metric for comparison was the power consumption of the various cycles, as represented by the system COP. Each cycle was required to deliver subcooled R-134a to an evaporator and had to reject heat at 40°C. Results show that a two-loop system, in which a conventional vapor-compression loop is coupled thermally to a pumped loop that directly cools the high-heat-flux chip, consumes much less energy than a conventional vapor-compression system. The simple vapor-compression cycle requires excessive energy consumption, largely because of the additional heat required to return the refrigerant to its vapor state before the compressor inlet.

Acknowledgment

This work is supported by the Office of Naval Research as a MURI award (Prime Award No. N00014-07-1-0723).

Nomenclature

$\dot{Q}$ = heat flow, kW
h = specific enthalpy, kJ/kg
$\dot{m}$ = mass flow rate, kg/s
$\dot{P}_{in}$ = total power input, kW
s = specific entropy, kJ kg^{-1} K^{-1}
T = temperature, °C
$\dot{W}$ = power input for compressors or pumps, kW
x = quality, %
η = isentropic efficiency for compressors or pumps

Subscripts

1, 2,…,8 = state points
A, B,…,D = state points
a, b,…,d = state points
add = additional heat required
com = compressor
cond = condenser
evap = evaporator
pump = pump
tec = thermoelectric

References

[1] Phelan, P. E., Chiriac, V. A., and Lee, T.-Y. T., 2002, "Current and Future Miniature Refrigeration Cooling Technologies for High-Power Microelectronics," IEEE Trans. Compon., Hybrids, Manuf. Technol., **25**, pp. 356–365.
[2] Phelan, P. E., Swanson, J., Chiriac, F., and Chiriac, V. A., 2004, "Designing a Mesoscale Vapor Compression Refrigerator for Cooling High-Power Microelectronics," ITHERM, Las Vegas, NV, Jun. 1–4, pp. 218–223.
[3] Mongia, R., Masahiro, K., DiStefano, E., Barry, J., Chen, W., Izenson, M., Possamai, F., Zimmermann, A., and Mochizuki, M., 2006, "Small Scale Refrigeration System for Electronics Cooling Within a Notebook Computer," ITHERM, San Diego, CA, May 30–Jun. 2, pp. 751–758.
[4] Trutassanawin, S., Groll, E. A., Garimella, S. V., and Cremaschi, L., 2006, "Experimental Investigation of a Miniature-Scale Refrigeration Systems for Electronics Cooling," IEEE Trans. Compon. Packag. Technol., **29**, pp. 678–687.
[5] Chiriac, V., and Chiriac, F., 2008, "An Overview and Comparison of Various Refrigeration Methods for Microelectronics Cooling," ITHERM, May 28–31, Orlando, FL, pp. 618–625.
[6] Chu, R. C., Simons, R. E., Ellsworth, M. J., Schmidt, R. R., and Cozzolino, V., 2004, "Review of Cooling Technologies for Computer Products," IEEE Trans. Device Mater. Reliab., **4**, pp. 568–585.
[7] Peeples, J. W., 2001, "Vapor Compression Cooling for High Performance Applications," Electronics Cooling, **7**, pp. 16–24.
[8] Nnanna, A. G. A., 2006, "Application of Refrigeration System in Electronics Cooling," Appl. Therm. Eng., **26**, pp. 18–27.
[9] Lee, J., and Mudawar, I., 2006, "Implementation of Microchannel Evaporator for High-Heat-Flux Refrigeration Cooling Applications," ASME J. Electron. Packag., **128**, pp. 30–37.
[10] Lee, J., and Mudawar, I., 2009, "Low-Temperature Two-Phase Micro-Channel Cooling for High-Heat-Flux Thermal Management of Defense Electronics," IEEE Trans. Compon. Packag. Technol., **32**, pp. 453–465.
[11] Lee, J., and Mudawar, I., 2008, "Fluid Flow and Heat Transfer Characteristics of Low Temperature Two-Phase Micro-Channel Heat Sinks—Part 1. Experimental Methods and Flow Visualization Results," Int. J. Heat Mass Transfer, **51**, pp. 4315–4326.
[12] Lee, J., and Mudawar, I., 2008, "Fluid Flow and Heat Transfer Characteristics of Low Temperature Two-Phase Micro-Channel Heat Sinks—Part 2. Subcooled Boiling Heat Transfer and Pressure Drop," Int. J. Heat Mass Transfer, **51**, pp. 4327–4341.
[13] Mudawar, I., and Bowers, M. B., 1999, "Ultra-High Critical Heat Flux (CHF) Subcooled Water Flow Boiling–I: CHF Data and Parametric Effects for Small Diameter Tubes," Int. J. Heat Mass Transfer, **42**, pp. 1405–1428.
[14] Wojtan, L., Revellin, R., and Thome, J. R., 2006, "Investigation of Saturated Critical Heat Flux in a Single, Uniformly Heated Microchannel," Exp. Therm. Fluid Sci., **30**, pp. 765–774.
[15] Koşar, A., and Peles, Y., 2007, "Critical Heat Flux of R-123 in Silicon-Based Microchannels," ASME J. Heat Transfer, **129**, pp. 844–851.
[16] Roday, A. P., and Jensen, M. K., 2009, "A Review of the Critical Heat Flux

Condition in Mini- and Microchannels," J. Mech. Sci. Technol., **23**, pp. 2529–2547.
[17] Bertsch, S. S., Groll, E. A., and Garimella, S. V., 2008, "Refrigerant Flow Boiling Heat Transfer in Parallel Microchannels as a Function of Local Vapor Quality," Int. J. Heat Mass Transfer, **51**, pp. 4775–4787.
[18] Çengel, Y. A., and Boles, M. A., 2008, *Thermodynamics: An Engineering Approach*, 6th ed., McGraw-Hill, Boston, MA, pp. 623–660.
[19] Riffat, S. B., and Ma, X., 2004, "Improving the Coefficient of Performance of Thermoelectric Cooling Systems: A Review," Int. J. Energy Res., **28**, pp. 753–768.